2014

An agent-based movement model to assess the impact of landscape fragmentation on disease transmission

Jeff A. Tracey
Colorado State University - Fort Collins, jeff.a.tracey@gmail.com

Sarah N. Bevins
Colorado State University - Fort Collins, Sarah.N.Bevins@aphis.usda.gov

Sue VandeWoude
Colorado State University - Fort Collins, sue.vandewoude@colostate.edu

Kevin R. Crooks
Colorado State University - Fort Collins, kevin.crooks@colostate.edu

esa

ECOSPHERE

An agent-based movement model to assess the impact of landscape fragmentation on disease transmission

JEFF A. TRACEY,[1,3,]† SARAH N. BEVINS,[2] SUE VANDEWOUDE,[2] AND KEVIN R. CROOKS[1]

[1]*Department of Fish, Wildlife, and Conservation Biology, Colorado State University, Fort Collins, Colorado 80523-1474 USA*
[2]*Department of Microbiology, Immunology, and Pathology, Colorado State University, Fort Collins, Colorado 80523-1601 USA*

Citation: Tracey, J. A., S. N. Bevins, S. VandeWoude, and K. R. Crooks. 2014. An agent-based movement model to assess the impact of landscape fragmentation on disease transmission. Ecosphere 5(9):119. http://dx.doi.org/10.1890/ES13-00376.1

Abstract. Landscape changes can result in habitat fragmentation and reduced landscape connectivity, limiting the ability of animals to move across space and altering infectious disease dynamics in wildlife. In this study, we develop and implement an agent-based model to assess the impacts of animal movement behavior and landscape structure on disease dynamics. We model a susceptible/infective disease state system applicable to the transmission of feline immunodeficiency virus in bobcats in the urbanized landscape of coastal southern California. Our agent-based model incorporates animal movement behavior, pathogen prevalence, transmission probability, and habitat fragmentation to evaluate how these variables influence disease spread in urbanizing landscapes. We performed a sensitivity analysis by simulating the system under 4200 different combinations of model parameters and evaluating disease transmission outcomes. Our model reveals that host movement behavior and response to landscape features play a pivotal role in determining how habitat fragmentation influences disease dynamics. Importantly, interactions among habitat fragmentation and movement had non-linear and counter-intuitive effects on disease transmission. For example, the model predicts that an intermediate level of non-habitat permeability and directionality will result in the highest rates of between-patch disease transmission. Agent-based models serve as computational laboratories that provide a powerful approach for quantitatively and visually exploring the role of animal behavior and anthropogenic landscape change on contacts among agents and the spread of disease. Such questions are challenging to study empirically given that it is difficult or impossible to experimentally manipulate actual landscapes and the animals and pathogens that move through them. Modeling the relationship between habitat fragmentation, animal movement behavior, and disease spread will improve understanding of the spread of potentially destructive pathogens through wildlife populations, as well as domestic animals and humans.

Key words: agent-based model; animal movement; bobcat; epidemiology; habitat fragmentation; individual-based model; landscape connectivity; *Lynx rufus*; wildlife disease.

Received 2 December 2014; accepted 23 April 2014; final version received 26 August 2014; **published** 29 September 2014. Corresponding Editor: N. T. Hobbs.

[3] Present address: San Diego Field Station, Western Ecological Research Center, U.S. Geological Survey, 4165 Spruance Road, Suite 200, San Diego, California 92101 USA.

† **E-mail:** jeff.a.tracey@gmail.com

INTRODUCTION

Emerging infectious diseases are a serious public health threat, with zoonotic pathogens accounting for approximately 60% of emerging diseases (Woolhouse and Gowtage-Sequeria

2005, Jones et al. 2008). Ecological processes combined with anthropogenic landscape changes may alter disease distribution, prevalence, and dynamics. As examples, dam building has led to increased human schistosomiasis infections (Picquet et al. 1996), forest fragmentation and the resultant change in rodent host populations has been linked to Lyme disease risk in the US (LoGiudice et al. 2003), and deforestation has increased malaria-transmitting mosquito habitat in the Amazon (Vittor et al. 2009). Pathogens are also a concern for wildlife conservation (McCallum and Dobson 2002, Smith et al. 2009).

Contact between susceptible and infective individuals within a population is a critical process in transmission of many diseases and is influenced by multiple factors, including individual condition, movement behavior, social interactions, and landscape features. Habitat fragmentation, the parcelization of larger habitat patches into smaller remnants, can alter functional landscape connectivity, the flow of organisms across a landscape (Crooks and Sanjayan 2006). Fragmentation often occurs as a result of habitat removal, but can result from other landscape changes, such as the construction of fences or other features that restrict animal movement. In turn, habitat fragmentation and restricted landscape connectivity can alter inter- and intra-specific interactions and the potential of disease spread (Hess 1996, McCallum and Dobson 2002, McCallum and Dobson 2006). In many regions, urbanization is a leading cause of habitat fragmentation and species endangerment (McKinney 2002, McDonald et al. 2008). For some species, urbanization can lead to reduced home range sizes and territories that overlap more when compared to rural locations (Riley 2006). The resultant increase in contact rates can lead to changes in disease transmission patterns in urbanizing landscapes (Bevins et al. 2012, Lee et al. 2012); increased contact between wild and domestic animals in urban areas can also introduce novel disease (Williams et al. 1988, Laurenson et al. 1998).

The effects of habitat fragmentation on pathogen dynamics have been explored theoretically (Hess 1996, McCallum and Dobson 2002, 2006), with differing predictions. A highly fragmented landscape has been shown to reduce between-patch transmission by preventing dispersal between habitat patches (Hess 1996). Habitat fragmentation could also limit within-patch transmission by restricting population numbers to levels below threshold values needed by pathogens to persist (Hess 1996). Alternatively, a highly fragmented landscape could also increase transmission by increasing the density of individuals occupying a habitat patch (McCallum and Dobson 2002). In this paper, we use agent-based modeling to explore the potential effects of animal movement behavior and landscape structure on the spread of a simulated disease among host animals in landscapes impacted by varying degrees of urban fragmentation.

Agent-based modeling is a "bottom-up" approach that simulates sensing of the external environment (e. g., the local landscape), information processing, behavior, and interactions of discrete decision-making entities, called "agents" (Bankes 2002). Herein, we use agent to refer to the discrete decision-making entities in our models (i.e., animals), in contrast to "pathogen," which refers to the disease-causing microorganisms the animals carry and transmit. "Emergent" properties are system-level patterns that arise from interactions between agents and their environment and are characteristic of complex biological systems. These system-level behaviors are difficult to infer from the behavior of individual agents, but agent-based models (ABMs) offer a way to discern such large-scale patterns and emergent phenomena (Bankes 2002). As such, ABMs can be regarded as computational laboratories (Valbuena et al. 2009) that are used to conduct "in silico" experiments (Green et al. 2005) to aid in understanding systems whose scale make them difficult to study empirically. Although traditional differential equation models have provided insight into disease dynamics (Grenfell and Dobson 1995), such models necessarily simplify behavior and interactions between individuals at a local level in order to achieve a mathematically tractable description of population-level dynamics. ABMs offer a powerful method to explore disease dynamics by focusing on interactions of agents to determine effects on the system as a whole, thereby providing a useful approach for modeling the role of host behavior in a spatial context (Auchincloss and Diez Roux 2008). ABMs

have been used to investigate disease dynamics in wildlife (for example Thulke et al. 1999, Fa et al. 2001), including ABMs that have incorporated spatial behaviors (Jeltsch et al. 1997). Our study provides an extensive investigation of the relation between landscape fragmentation and movement behavior using ABMs.

Our agent-based modeling work is motivated by a long-term study of the ecology and disease dynamics of bobcats in urban environments in coastal southern California. Bobcats are wide-ranging, fragmentation-sensitive carnivores; thus, they are excellent focal species for investigations of the impacts of urbanization in southern California and elsewhere (Laurenson et al. 1998, Crooks 2002, Tigas et al. 2002, Riley et al. 2003, Ruell et al. 2009). Intensive radio- and GPS telemetry studies have been conducted on the spatio-temporal movement patterns and habitat use of bobcats in urban areas near Los Angeles (Riley et al. 2003, Riley et al. 2010, Tracey et al. 2013); these animals have also been screened for seroprevalence of multiple pathogens, including feline immunodeficiency virus (FIV; Franklin et al. 2007, Bevins et al. 2012, Lee et al. 2012).

Feline immunodeficiency virus is a naturally occurring lentivirus in many felid species, including bobcats (Franklin et al. 2007). It is directly transmitted, with two states (S = susceptible and I = infective) and one state transition (from S to I). The pathogen typically does not cause direct mortality or effect fitness in non-domestic felids, and the feline host remains persistently infective (VandeWoude and Apetrei 2006). Seroprevalence in domestic cats is typically low, often less than 10% (Courchamp et al. 2000, VandeWoude and Apetrei 2006), whereas seroprevalence values in wild non-domestic felid populations are highly variable (Franklin et al. 2007). Disease spread in our model is motivated by FIV because its characteristics (Bevins et al. 2012) make it a relatively simple infection to model. It should be noted, however, that the ABM approach we have developed can be readily adapted to other diseases with different states, transitions, modes of transmission, and effects on the host.

We design and build an Ecological Infectious Disease ABM (EID-ABM) to evaluate the impacts of urban fragmentation on animal movement and disease spread. Design specifications required the ABM to permit exploration of interactions among landscape structure, animal movement, and disease dynamics in a simulated environment. In addition to focusing on habitat fragmentation and disease transmission, we required: (1) an explicit representation of landscape structure, and, (2) simulated bobcat movement in response to landscape structure representing functional connectivity among habitat patches and contacts between simulated bobcats. This version of the model intentionally omits specific details, such as demographic events and life history, to better understand the effects of movement behavior, landscape, and disease in the ABM. We analyzed the behavior of the EID-ABM by sensitivity analysis of the model responses, including disease prevalence, disease transmission within habitat patches, and disease transmission between habitat patches.

This analysis addressed three critical questions regarding the effects of landscape structure and animal movement behavior on disease spread. First, how does habitat fragmentation (landscape structure) affect the spread of an SI disease within and between habitat patches? We expected a priori that more fragmentation would increase transmissions within habitat patches and decrease transmissions between habitat patches. Second, how does movement behavior affect the spread of an SI disease within and between habitat patches? We hypothesized that more directional movement, approximating a dispersing animal, would result in more between-patch transmission and less within-patch transmission compared to a point attraction movement rule, typifying an animal with a resident home range. Third, how does habitat fragmentation and move behavior interact to affect the spread of an SI disease within and between habitat patches? We expected that behavioral avoidance of the matrix between habitat fragments (i.e., "non-habitat") would increase within-patch transmission but decrease it between patches. In this paper, we use the EID-ABM, based on bobcats in a landscape fragmented by urban development, to evaluate these questions and identify the conditions under which the hypotheses we pose hold true. In the discussion we discuss the results in light of findings from empirical studies of felid diseases in southern California.

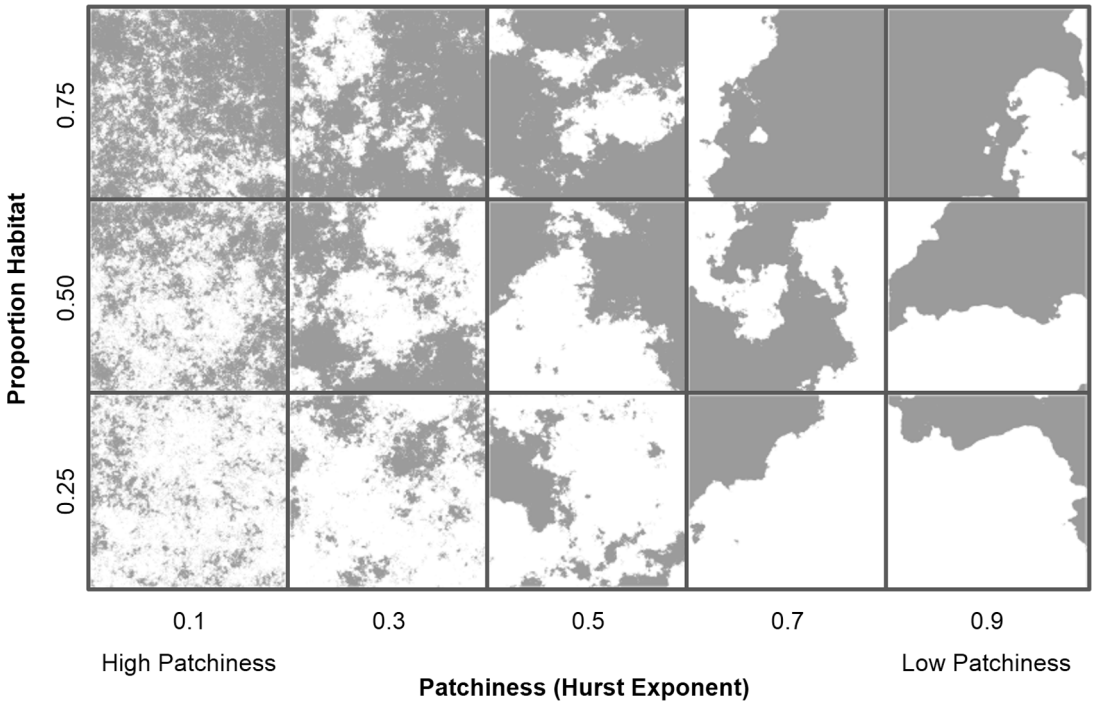

Fig. 1. Simulation of landscapes that varied in degree of habitat fragmentation in the EID-ABM. Fractal landscapes generated using the midpoint displacement algorithm along a gradient of habitat loss (proportion of habitat) and habitat patchiness (Hurst exponent) simulates the processes of habitat fragmentation. Habitat is shown in gray and non-habitat in white. Habitat patchiness increases as the Hurst exponent decreases. Habitat loss and habitat patchiness vary independently in the models; in real landscapes, however, habitat fragmentation typically includes the simultaneous loss of habitat and parcelization of remaining patches. For our study area in coastal southern California, we estimated the proportion of habitat to be 0.3126 and the Hurst exponent to be 0.5845, which most closely corresponds to the panel in the middle column, bottom row.

Methods

We describe the components of the EID-ABM and simulation experiments to study the interactions of movement behavior, landscape structure, and disease transmission in a susceptible/infected (SI) disease. Additional details on the movement rules are in Appendix A, and additional resources are given as a Supplement.

Components of the EID-ABM

The Ecological Infectious Disease ABM (EID-ABM) is a spatially explicit, discrete-time model with six main components: (1) landscapes (Fig. 1), (2) susceptible or infected 'agents' representing individual bobcats (Fig. 2), (3) movement behavior rules used by agents to move across the landscape (Table 1), (4) a simple SI disease, (5) a dynamic contact network that connects agents based on the distance between them (Fig. 2), and (6) a disease transmission network that stores information on transmission events (Fig. 2).

Landscapes.—In order to control the patchiness and amount of habitat in the model, we simulated land cover using a fractal-based algorithm, the mid-point displacement method (Turner et al. 2001). This algorithm allowed us to independently vary the proportion of habitat (p, such that $0 \leq p \leq 1$) and habitat patchiness controlled by the Hurst exponent parameter (H, such that $0 \leq H \leq 1$). Habitat patchiness decreases as the Hurst exponent (H) decreases (see Fig. 1, Table 2). These gradients of proportion of habitat and degree of habitat patchiness approximate patterns seen in urbanizing landscapes, spanning relatively unfragmented systems with large intact habitat blocks to highly

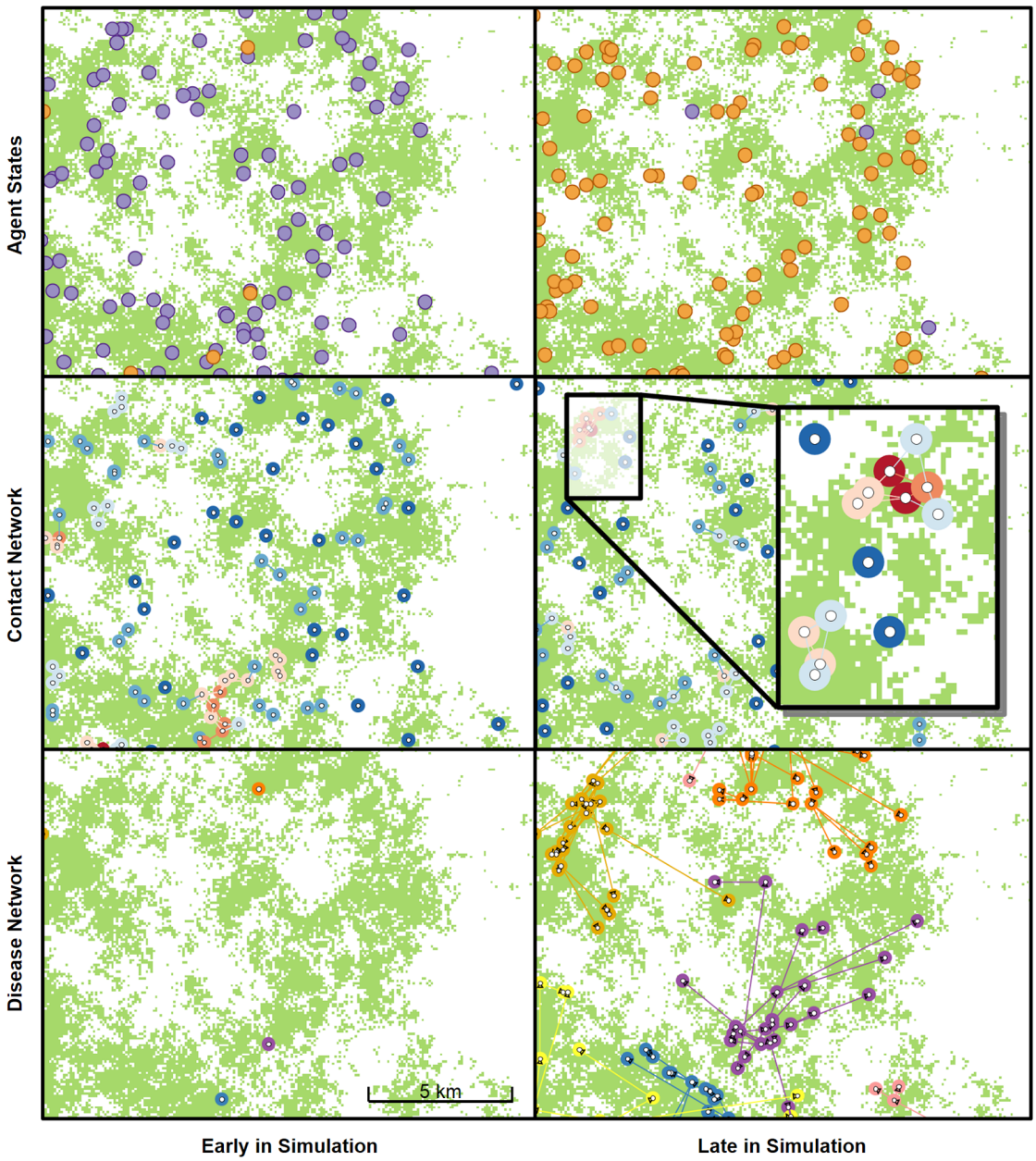

Fig. 2. The EID-ABM tracks changes in location, susceptibility, contact, and disease transmission over time. This visualization of the EID-ABM shows the locations of infective (orange) and susceptible (purple) simulated bobcats (top row), contact networks (middle row), and disease transmission networks (bottom row). The figure shows images from the display in the early (left column) and final (right column) stages of a simulation. In contact networks, dark blue nodes are locations of animals with no neighbors. As the color of the nodes change from dark blue to light blue to light orange to dark orange, the simulated bobcats (agents) have more neighbors with whom they are in contact. If the disease is transmitted from one agent to another, the location of the transmission is shown as a node (point) in the disease network. Nodes in the disease network are displayed in different colors, each color corresponding to a different agent that was initially infective at the beginning of the simulation. This allows a visual trace of disease spread across time and space, and among habitat patches.

Table 1. A listing of the 28 movement rules considered in the sensitivity analysis. The equations for the movement rules are provided in Appendix A.

Rule	Description	Variations
SRW, $n = N$	Simple random walk with non-habitat permeability n, which controls the probability of movement through non-habitat.	SRW, $n = 0.0$ SRW, $n = 0.01$ SRW, $n = 0.05$ SRW, $n = 1.0$
$CRW_{k=K}$, $n = N$	Correlated random walk with concentration k and non-habitat permeability n. The concentration k controls the directionality of the movement.	$CRW_{k=2}$, $n = 0.0$ $CRW_{k=2}$, $n = 0.01$ $CRW_{k=2}$, $n = 0.05$ $CRW_{k=2}$, $n = 1.0$ $CRW_{k=5}$, $n = 0.0$ $CRW_{k=5}$, $n = 0.01$ $CRW_{k=5}$, $n = 0.05$ $CRW_{k=5}$, $n = 1.0$ $CRW_{k=10}$, $n = 0.0$ $CRW_{k=10}$, $n = 0.01$ $CRW_{k=10}$, $n = 0.05$ $CRW_{k=10}$, $n = 1.0$
$PA_{d=D}$, $n = N$	Point attraction with non-habitat permeability n, location parameter d, $b = 0.1$, $k_{max} = 1.0$. The parameter k_{max} sets the maximum attraction to the central location and b sets the shape of the curve controlling the change in attraction as the distance to the central location increases. The parameter d relates to the radius of the area around the agent's initial location within which it moves freely.	$PA_{d=500}$, $n = 0.0$ $PA_{d=500}$, $n = 0.01$ $PA_{d=500}$, $n = 0.05$ $PA_{d=500}$, $n = 1.0$ $PA_{d=1000}$, $n = 0.0$ $PA_{d=1000}$, $n = 0.01$ $PA_{d=1000}$, $n = 0.05$ $PA_{d=1000}$, $n = 1.0$ $PA_{d=1500}$, $n = 0.0$ $PA_{d=1500}$, $n = 0.01$ $PA_{d=1500}$, $n = 0.05$ $PA_{d=1500}$, $n = 1.0$

fragmented areas composed of numerous, small habitat remnants (Fig. 1). In real landscapes, habitat fragmentation due to human-caused landscape change often results in a simultaneous decrease in proportion habitat and increase in habitat patchiness; however, in our simulated landscapes, we varied these two properties of the landscapes independently. The land cover generated by this algorithm is represented by a raster. Each raster cell is 100 meters by 100 meters. Landscapes consist of 500 cells by 500 cells, or 50 km by 50 km. Each cell in a land cover raster is

Table 2. Parameters for agent-based model to predict animal movement and disease transmission in urban landscape. Parameters related to the scale of the landscape, time in the simulation, and overall density of agents per unit area of habitat were not varied in the simulations. Parameters that control habitat proportion and patchiness, movement rule, non-habitat permeability, initial disease prevalence, and probability of disease transmission were varied, resulting in 4200 different parameter combinations used in the sensitivity analysis. See text for details.

Parameter	Description	Type	Value
N_{real}	number of realizations	fixed	500
C_{size}	length of the side of a raster cell in meters	fixed	100 m
L_{size}	simulated landscape height and width in kilometers	fixed	50 km
T_{step}	length of a time step in days	fixed	0.0208333 d
T_{max}	time duration of simulation in days	fixed	200 d
A_{dens}	density of simulated bobcats (agents/km^2 of habitat)	fixed	0.35
P	proportion habitat	variable	0.1, 0.3, 0.5, 0.7, 0.9
H	Hurst exponent (habitat patchiness)	variable	0.1, 0.3, 0.5, 0.7, 0.9
MR	move behavior rule	variable	see Table 1
N	non-habitat permeability	variable	0.0, 0.01, 0.1, 1.0
I_{init}	initial proportion of individuals infective	variable	0.01, 0.05
P_{trans}	probability of disease transmission	variable	0.01, 0.1, 0.333

identified as habitat (the value for cell i is $h_i = 1$) or non-habitat (the value for cell i is $h_i = 0$).

Habitat patches are uniquely identified by a patch flooding algorithm. Two habitat cells in the land cover raster are considered connected if they are adjacent in either a cardinal or diagonal direction. This is the same neighborhood used in the movement rules, so an individual can move to any cell in the patch without entering non-habitat. Each patch is assigned a unique ID number in a second raster equal in size to the land cover raster. This allows us to uniquely identify each patch, calculate the patch characteristics, and track movements of agents and the disease between patches. The landscape affects (1) the abundance of agents, (2) the initial distribution of agents, and (3) agent movement decisions.

To facilitate comparison between simulated and actual landscapes, we computed the proportion of habitat and the fractal dimension of habitat patches for our southern California study area in coastal Orange County south of Los Angeles where we have conducted GPS telemetry studies on bobcats since 2002 (Riley et al. 2010, Tracey et al. 2013). Land cover data for our study area were compiled from land cover and impervious surface data from the National Land Cover Database (NLCD; Homer et al. 2004) and land use from the Southern California Association of Governments (SCAG, http://www.scag.ca.gov/; Appendix B: Fig. B1). Cells that were not classified as urban, agriculture, roads, or water were reclassified as habitat and all others were reclassified as non-habitat (see Supplemental Material). We calculated the proportion habitat (p) by dividing the number of habitat cells by the number of total cells. Using the R package SDMTools (VanDerWal et al. 2012), we calculated the fractal dimension (D) of the habitat patches, and then calculated the Hurst exponent as $H = 2 - D$ (see Appendix B).

Agents.—Agents are simulated bobcats. Our agents are reactive (Gimblett 2002); an agent's behavior is entirely determined by their movement behavior rule, which contains a stochastic element and landscape context. Each individual has a unique ID number and a point (x, y coordinates) for current location. Each agent also has a move behavior rule, a contact network node, and a disease network node. In this version of the model, we do not include demographic events, such as birth or death, life history stages, or goal-oriented behavior.

Move behavior rules.—Agents moved according to behavioral rules with properties similar to those of bobcats, including both territorial and dispersal movements (Table 1). The movement rules have two components: directionality and non-habitat permeability. Data gathered from studies of radio- and GPS-collared bobcats in the region (Riley et al. 2003, Riley et al. 2010, Tracey et al. 2013; J. A. Tracey, *unpublished data*) informed the three types of directionality used in the move behavior rules (Table 1): a simple random walk (SRW rule), a correlated random walk (CRW rule), and point attraction (PA rule). Movement behaviors form a gradient from locally restricted movement, similar to adult bobcats that have a home range or territory (PA rule), to simple random walk movement (SRW rule), to correlated random walk movements that cover large areas and are similar to dispersal movements of sub-adult bobcats (CRW rule). Additionally, we varied the degree of directionality in the CRW rule by using concentration parameter values of $k = 2$, 5, 10, where directionality increases with increasing k. We also varied the radius parameter of the locally-restricted movements in the PA rule, with location parameter $d = 500$, 1000, 1500 m representing increasing home range sizes that encompass those recorded for radio-collared bobcats in the region (mean radius 702.4 m females, 1010.8 m males; Riley et al. 2003, Ruell et al. 2009). Hence, movement rules approximate the basic movement patterns likely exhibited by bobcats in various life history stages. The probability that a simulated bobcat will leave habitat and enter non-habitat when it encounters a patch boundary is controlled by the non-habitat permeability parameter (n, Tables 1 and 2). In this case, non-habitat can be thought of as the developed urban matrix surrounding natural habitat patches. The non-habitat permeability parameter (n) ranges from 0.0, which results in complete avoidance of urban areas, to 1.0, where urban areas are completely permeable and simulated bobcats make no distinction between habitat and non-habitat.

During simulations, agent locations are restricted to the center of the raster cells. An agent

may decide to remain in the raster cell they currently occupy or move to one of eight neighboring cells, i.e., its Moore neighborhood (Stauffer and Aharony 1994). Landscape boundaries are reflective so that agents are confined to the landscape and the overall density of agents remains constant. All movement rules assign a probability of selecting each of the nine cells. Each rule may be used interchangeably by the agent; however, every agent uses the same form of the rule during a simulation in the current model configuration. Different rules will store different data (parameters and state variables) and implement rule-specific movement decisions.

SI disease.—We use a simple directly transmitted disease with two states, susceptible (S) and infective (I), representative of feline immunodeficiency virus (FIV; Fig. 2). FIV is found in many felid species, including bobcats (Franklin et al. 2007, Bevins et al. 2012) and is transmitted via exchange of bodily fluids, for example through aggressive or mating encounters. The pathogen typically does not cause direct mortality or affect fitness in non-domestic felids (Biek et al. 2006), and the feline host remains persistently infective (VandeWoude and Apetrei 2006). The simulated disease has no direct effect on an agent other than changing the disease state stored in the agent's disease network node, and there is no recovery/resistant stage nor a return to a susceptible state. Consequently, the infective stage is an absorbing state and disease prevalence cannot decrease in our simulated population.

Contact network.—The contact network connects agents within a maximum distance of each other and the network is updated each time step to account for changes in agent locations (Fig. 2). Maximum distance in the current model is set to 50 m; agents must be in the same cell to be connected. Disease spread from infective to susceptible agents is through the connections (edges) in the contact network. A contact network node has a reference to the agent that owns it and references to contact network edges. A contact network edge is directed and has references to the nodes it connects (from node, to node) and the Euclidean distance between the nodes based on corresponding agent locations.

Disease transmission network.—The disease transmission network tracks disease spread across agents, time, space, and habitat patches (Fig. 2). At the start of a simulation, the nodes in the network correspond to each initially infective individual and none of the nodes in the disease transmission network are connected (Fig. 2). Each tree, rooted in a node that corresponds to an initially infective agent, grows by accretion as the infection spreads. When an infective agent transmits the disease to a susceptible agent, their corresponding nodes in the disease transmission network are connected with a directed edge from the infective to the susceptible agent's node. Disease transmission network nodes store information on unique node ID, disease transmission tree ID, agent disease state, the time the corresponding agent was infected, infection location, and the ID number of the habitat patch in which the agent was infected. The directed edges also store data on the distance between the location where the agent became infective, the location where it transmitted the disease to the susceptible agent, and elapsed time between these transmission events. Thus, the disease network can be used to both quantify and visualize how an infection spreads across both the simulated fragmented landscape and the population of agents. An example is given in Fig. 2, where each tree is displayed with a different color. As the disease is transmitted from one agent to another, these trees grow, and the new nodes of the trees are displayed at the location where transmission events occurred.

Simulation experiments using the EID-ABM

In order to understand the system-level behavior and address our research questions, we performed a visual sensitivity analysis of our ABM by keeping some parameters fixed (Table 2), performing parameter sweeps over a range of values for the remaining parameters (Tables 1 and 2), and collecting outputs for model response. Based on bobcat density estimates in coastal southern California (Ruell et al. 2009), we introduced simulated bobcats onto the landscape (Fig. 2) at a constant density of 0.35 agents per square kilometer of habitat. Time step size ($T_{\text{step}} = 30$ minutes), time duration of simulation ($t_{\max} = 200$), landscape grain (100 m by 100 m) and extent (50 km by 50 km), and number of realizations ($N_{\text{real}} = 500$) were also constant in all cases. We varied: (1) the proportion of habitat

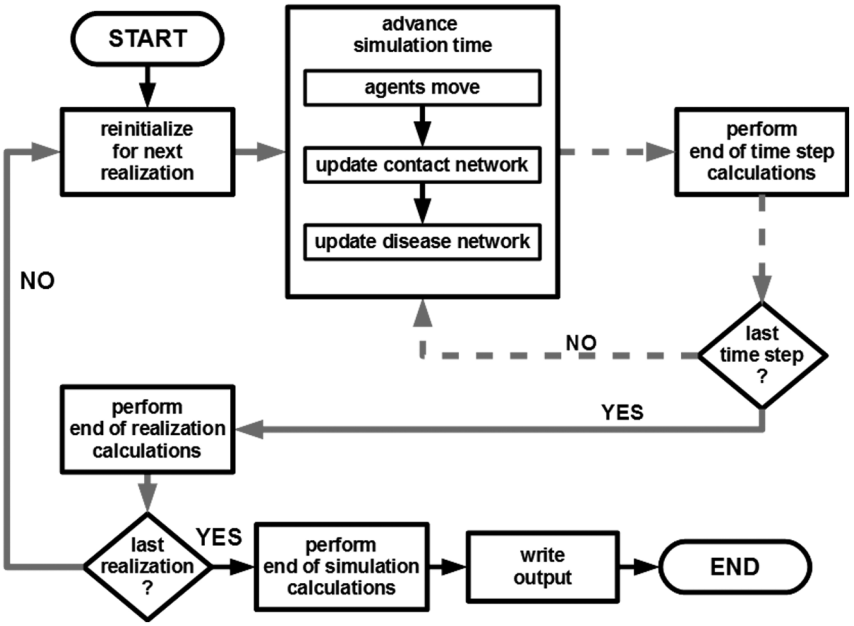

Fig. 3. The computational process used to generate output from the EID-ABM. The flow chart illustrates processes (rectangles) and decisions (diamonds) arranged in two main loops: 30-minute time steps (gray dashed arrows) and realizations consisting of 9600 time steps (gray arrows). During each time step, each simulated bobcat makes a move and updates its location. Once agent locations are updated, the contact network and then the disease network are updated. After 500 realizations, the output for a given combination of parameters is written to a file.

(p) and the Hurst exponent (H) that determines habitat patchiness; (2) movement rules used by agents, including the form of the rule (PA, SRW, and CRW) and rule-specific parameters; (3) non-habitat permeability (n); (4) disease transmission probability (P_{trans}); and (5) initial proportion infective (I_{init}). The values used are listed in Tables 1 and 2. As a result, we evaluated the behavior of the EID-ABM under 4200 different model parameter combinations (Table 1 and 2; Fig. 3). Each realization contained an average of 438 simulated bobcats—dependent upon proportion of habitat in a landscape—each making 9600 simulated moves over the course of 200 days of continual movement.

At the beginning of each realization, the landscape and agents are initialized. Generating a fractal landscape is computationally expensive, so we generated a new fractal landscape, ran 20 realizations on this landscape, and then repeated the process. After all 500 realizations for a scenario were run, a total of 25 fractal landscapes were generated. Once the landscape was initialized, agents are introduced to the landscape in either the susceptible or infective state (Fig. 2). Initial prevalence parameters in this simulation were set at 1.0% or 5.0% based upon previously reported FIV infection rates (Troyer et al. 2005, Bevins et al. 2012; Table 2).

Within a single time step, the agents move, the contact network is updated, and then the disease network is updated (see Fig. 3). Agent locations are updated asynchronously, with the order in which the agents are updated randomized at each time step. Once the agents are at their new locations, the old edges of the contact network are removed, and new ones are created (Fig. 2). Simulated pathogen transmission from infective to susceptible agents occurred following contact (Fig. 3). If the susceptible agent is in contact with at least one infective agent, a probability that it would acquire the infection from an infective contact is calculated from the disease transmission probability (P_{trans}) and the number of infective neighbors as one minus the probability of not being infected by any infective neighbor.

Then, a random draw (a Bernoulli trial) using this probability determines if the susceptible individual becomes infective. The probability of transmission when two simulated bobcats come in contact was set at 0.01, 0.10, or 0.333 (Table 2), based upon FIV transmission rates among domestic cats (Courchamp et al. 2000). If the agent becomes infective, the source of infection is determined by randomly selecting an infective agent with whom the agent was in contact. Finally, the two agents are connected by a directed edge from S to I in the disease network, and the information in the disease network nodes and edges updated (Fig. 2 and 3).

To quantify disease prevalence, we stored the proportion of infective agents (disease prevalence) at each time step. We calculate the mean, median, variance, 50% confidence interval (CI), and 95% CI for each trajectory. Because prevalence only increases in our simulations, we used mean prevalence at the final time step of the simulation as a metric of disease spread.

To further quantify disease spread, we also tracked disease transmission within and between each habitat patch using the patch raster and the disease network. For each scenario, we computed the mean, median, variance, 50% CI, and 95% CI for (1) the number of patches, (2) the area of the patches, (3) the proportion of secondary infections each initial infective produced within its "home" patch, (4) the proportion of secondary infections each initial infective produced in a patch other than its "home" patch, (5) the proportion of disease transmissions that occurred outside of patches, (6) the time between transmissions, (7) the distance between transmissions, (8) the proportion of patches in which disease transmissions occurred, and (9) the proportion of the total habitat area represented by patches in which disease transmissions occurred.

Using the disease network, we identified disease transmission locations that occurred in the same habitat patch in which the initially infective individual started, those that occurred in different habitat patches, and those that occurred within the matrix outside of any habitat patch. The transmission events in a given tree in the disease network included those from one initially infective agent and all agents whose infection was traced back to that initially infective agent. We then computed the proportion of between-patch transmission events as the number of disease transmission events that occurred in habitat patches other than the starting habitat patch divided by the total number of disease transmission events. We used the proportion of between-patch transmissions as one metric to describe the spread of the disease across the landscape. Similarly, we computed the proportion of within-patch transmission events as the number of disease transmission events that occurred in the starting habitat patch divided by the total number of disease transmission events. We used the proportion of within-patch transmissions as a metric to describe the extent to which the spread of the disease is confined to habitat patches. We visualized and analyzed the results of all 4200 parameter combinations (scenarios) using the R programs that we described above.

Because ABMs are capable of producing large quantities of output, analysis and interpretation of the results can be difficult. In our sensitivity analysis, a total of 2,100,000 realizations of the model were run, generating approximately 8.8 trillion individual moves and over 10 gigabytes of output data. We visualized simulation results for each response variable (proportion of between-patch transmissions, proportion of within-patch transmissions, and mean proportion infective) as 'heat maps' that graphically summarized the output data across scenarios. We visualized and analyzed the results of the simulation version output using programs we wrote in the statistical programming language R (R Development Core Team 2007). The plots were produced within R using the facet grid layout and the tile geometry functions in the ggplot2 package (Wickham 2009). Using this approach, patterns in model responses could be evaluated across a large number of parameter combinations for proportion habitat, habitat patchiness, non-habitat permeability, and movement rules by observation of heat map patterns. This provided an effective method for reviewing and interpreting results gleaned from the very large datasets that emerged from the ABM simulations.

Results

Here we describe simulation results related to: (1) between-patch transmission: transmission of

infection from an infective to a susceptible agent in a habitat patch other than the patch in which the infection was introduced, (2) within-patch transmission: transmission of infection from an infective to a susceptible agent in the same habitat patch in which the infection was introduced, and (3) overall population prevalence: proportion of simulated bobcats infected at the final time step of the simulations. For our coastal Orange County study area in southern California, we estimated the proportion of habitat as $p = 0.3126$ and a Hurst exponent of $H = 0.5845$, which is comparable to the parameters we used in some scenarios (i.e., $p = 0.3$ and $H = 0.5$). A map of the habitat patches from our study site and simulated fractal landscapes created using the proportion of habitat and the Hurst exponent from the study area are given as an Appendix B: Fig. B1 and B2.

Between-patch disease transmission.—Overall, between-patch transmission increased with habitat patchiness and decreased with proportion of habitat (Fig. 4A–C). This pattern is related to how the landscape parameters affected the size, number, and isolation of habitat patches in the landscape as well as how agent movement behavior interacted with the landscape. When proportion of natural habitat was held constant, parcelization of the remaining habitat created numerous small, less-isolated fragments separated by shorter distances (Figs. 1, 5). Because the patches were smaller as patchiness increased, agents encountered patch boundaries more often, which lowered residency time within that patch and provided more opportunities to leave a patch and find new ones, necessary events for between-patch transmission (Fig. 5). Further, search time for new patches decreased as patches became less isolated, which in turn increased the rate at which an animal found a new patch in which to spread disease (Fig. 5). Although increasing the proportion of habitat also reduced patch isolation, it concurrently resulted in larger patches, thereby increasing residency time in patches and reducing between-patch transmission (Figs. 4A, 5).

Interactions between landscape structure and agent movement, as controlled by non-habitat permeability and move directionality, had non-linear and counter-intuitive effects on disease transmission among patches. An increase in non-habitat permeability reduces patch residency, which consequently increases patch emigration and new patch discovery (Fig. 5). Increased directionality of movement similarly reduces residency time in a habitat patch and also decreases search time for new patches (Fig. 5; Zollner and Lima 1999). Decreasing patch residency, however, also reduces the density of simulated bobcats in habitat patches, which leads to reduced contact rates, and reduces the amount of time animals spend in new patches, which limits disease spread.

These counter-acting relations suggest that there is an intermediate level of non-habitat permeability and directionality of movement that leads to the highest rates of between-patch transmission. Predictably, between-patch transmission was non-existent if non-habitat was impermeable and agents completely avoided it and never left patches ($n = 0$, Fig. 4B). However, between-patch transmission was also greatly reduced if there was no difference in permeability of habitat and non-habitat ($n = 1$, Fig. 4B), likely because residency time in patches is reduced and simulated bobcats are less aggregated in the landscape, leading to lower contact rates. Consequently, between-patch transmission was highest for habitats with very low non-habitat permeability ($n = 0.01$, Fig. 4B).

Between-patch transmission was also highest at intermediate levels of move directionality. The point-attraction (PA) and simple random walk (SRW) rules resulted in low between-patch transmission (Fig. 4C) because such movement rules restricted the degree to which agents emigrated from patches (Fig. 5). Conversely, the correlated-random walk (CRW) movement patterns, analogous to a dispersing individual, yielded the highest between-patch transmission. Between-patch transmission, however, was most frequent when agents moved according to the movement rule with intermediate (i.e., $CRW_{k=5}$) but not the highest (i.e., $CRW_{k=10}$) directionality, again likely reflecting the complex and conflicting trade-offs between patch residency, patch emigration and discovery, local agent density, and disease spread (Fig. 5).

Within-patch disease transmission.—In contrast to patterns evident for between-patch transmission, within-patch transmission events increased with proportion of habitat and decreased with

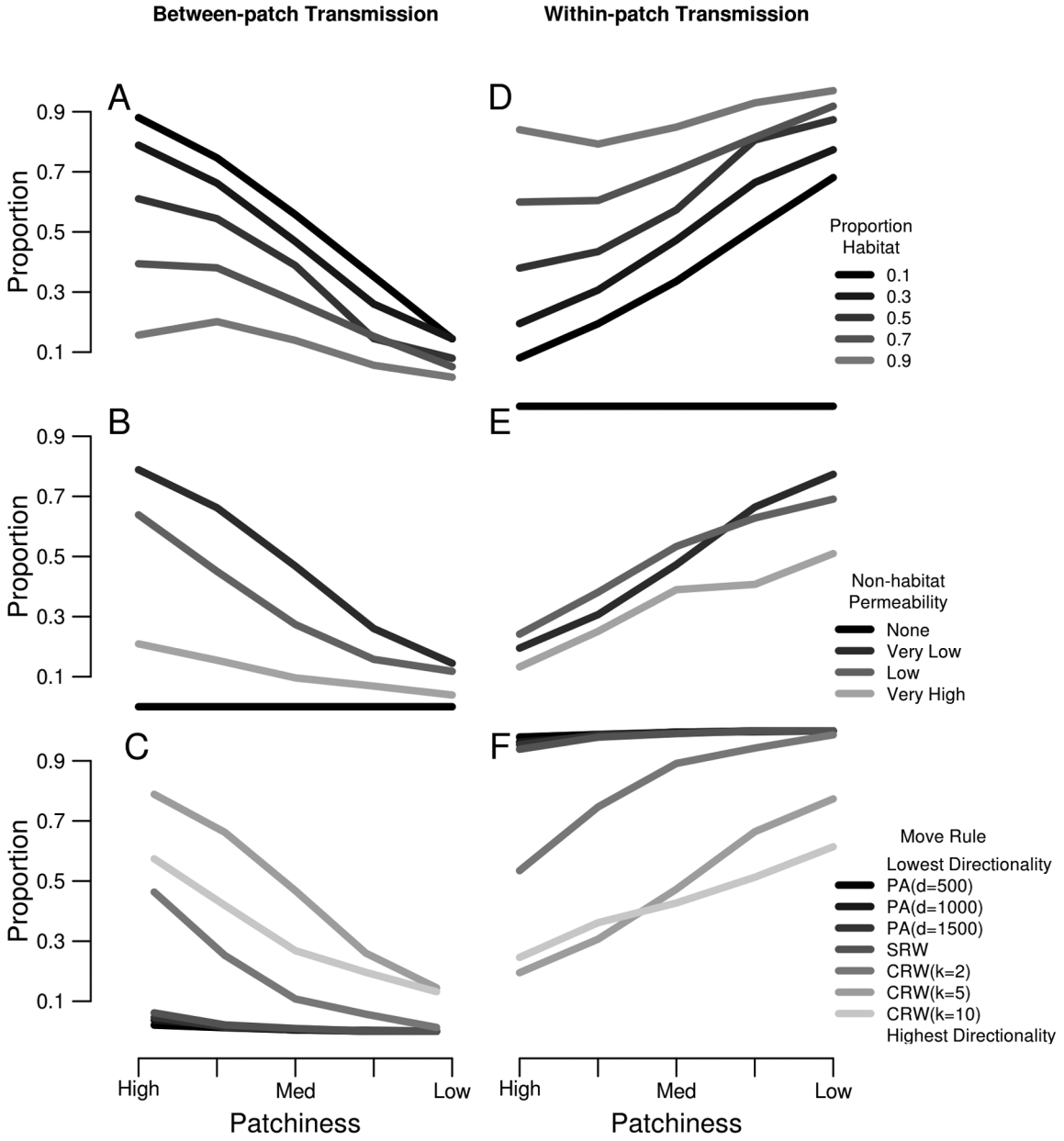

Fig. 4. Between-patch and within-patch disease transmission depends on habitat patchiness, proportion of habitat, non-habitat permeability, and movement rule. In all subplots, the degree of habitat patchiness is shown on the *x*-axis, the proportion of initially infective agents was 0.01, and the probability of disease transmission was 0.1. The proportion of between-patch transmissions (subplots A–C) and within-patch transmissions (subplots D–F) is shown on the *y*-axis. Subplots A and D illustrate the effects of proportion of habitat (move rule was $CRW_{k=5}$ and non-habitat permeability was 0.01). Subplots B and E illustrate the effects of non-habitat permeability (move rule was $CRW_{k=5}$ and non-habitat permeability was 0.3). Subplots C and F illustrate the effects of movement rule (proportion of habitat was 0.3 and non-habitat permeability was 0.01). For our study area in coastal southern California, we estimated the proportion of habitat to be 0.3126 and the Hurst exponent to be 0.5845. Non-habitat permeability was low to very low for the bobcats in our study area. Resident bobcats were most consistent with $PA_{d=1000}$, while dispersing bobcats were most consistent with $CRW_{k=3}$ or $CRW_{k=5}$.

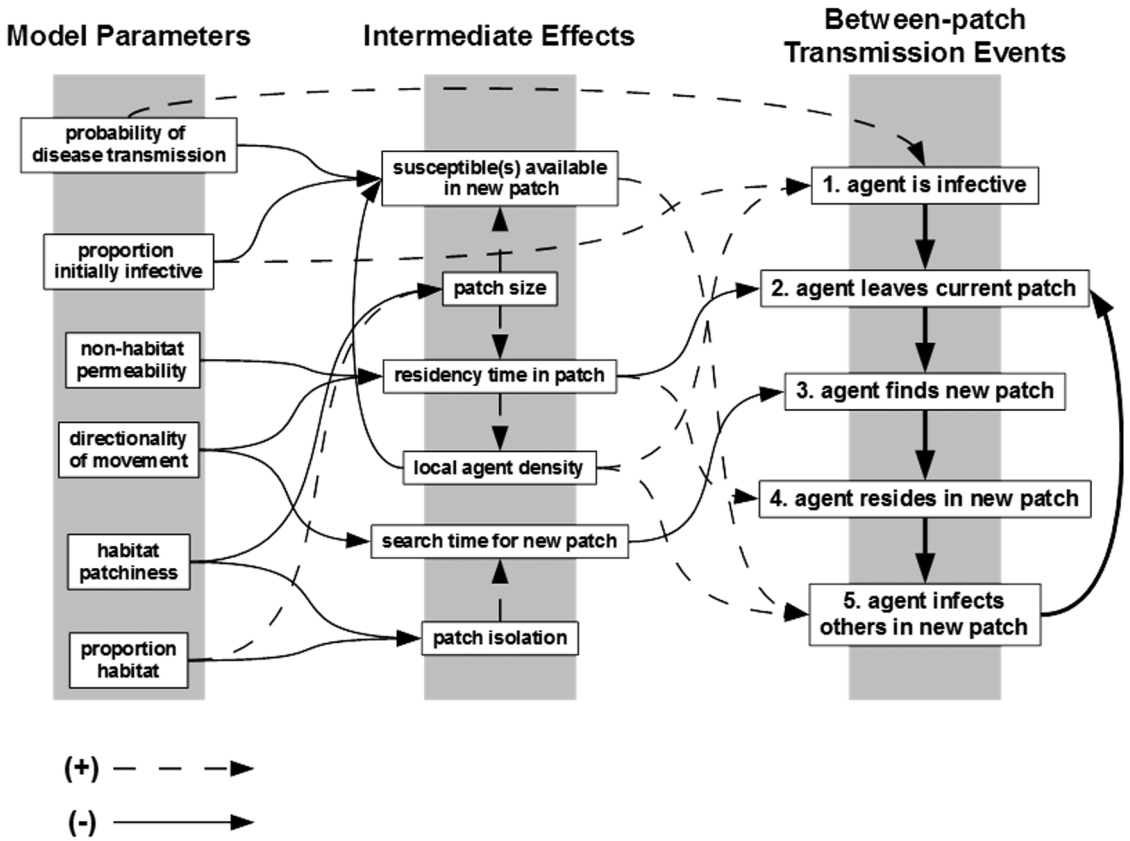

Fig. 5. Simple rules lead to complex interactions in the EID-ABM. Model parameters are depicted in the left column. Intermediate effects, which are the result of several model parameters, are described in the center column. Events that must occur to result in between-patch disease transmission (i.e., movement of an infected individual to a new patch and resulting sufficient contact with a susceptible individual in this patch) are listed in the right column. Arrows with thin, solid black lines indicate two elements that are positively related, with arrow directionality from the cause to the effect. If cause and effect are negatively related, the arrow has a thin, dashed black line. The events leading to between-patch transmission are connected by thick black arrows in temporal order.

habitat patchiness (Fig. 4D); within-patch transmission declined with habitat patchiness most rapidly when there was only limited habitat available. This pattern likely resulted from fewer opportunities for within-patch transmission in highly fragmented landscapes composed primarily of small habitat patches (Fig. 1).

Non-habitat permeability and directionality of movement had a strong effect on the proportion of within-patch transmissions (Fig. 4E, F), but in directions generally opposite to those for between-patch transmission. As might be expected, the proportion of within-patch transmissions increased as permeability of the matrix between fragments decreased (Fig. 4E). Correspondingly, if non-habitat was completely impermeable ($n = 0$), then all transmission events occurred in the habitat patches where the initially infective agents resided. While the results for within-patch and between-patch transmission were often inversely-related, some movement rules outperformed others in both types of transmission. For example, when habitat patchiness was medium-low or low, move rules with very low non-habitat permeability exceeded rules with low or high permeability in both the proportion of within-patch and between-patch transmissions (Fig. 4B, E). Also, the $CRW_{k=5}$ move rule out-per-

formed all others with respect to between-patch transmissions, but also out-performed $CRW_{k=10}$ in within-patch transmissions (Fig. 4C, F).

When we varied movement rules, the point-attraction (PA) and simple random walk (SRW) rules showed very high proportions of within-patch transmissions (Fig. 4F), again reflecting opposite patterns to those for between-patch transmission. In contrast, the dispersal-like correlated random walk (CRW) rules, particularly the two with the highest directionality ($CRW_{k=5}$ and $CRW_{k=10}$), resulted in lower proportions of within-patch transmissions. When habitat patchiness was medium-high to high, these two rules showed similar results, but as patchiness decreased, the rule with intermediate directionality ($CRW_{k=5}$) exceeded the rule with the highest directionality ($CRW_{k=10}$) in the proportion of within-patch transmissions (Fig. 4F). Importantly, high directionality resulted in agents spending more time in non-habitat, resulting in a higher proportion of transmission events in non-habitat.

Population level prevalence.—We summarize the overall ability of the infection to spread through the simulated population as prevalence, or mean proportion infective, expressed as the proportion of infective agents at the end of each realization of the simulation, averaged across all realizations using a given set of parameters.

In general, disease prevalence increased as the proportion of habitat increased (Fig. 6). The rate of change in prevalence was greater with the more directional movement rules, particularly CRW. In most cases, overall prevalence decreased with increasing habitat patchiness, except for the movement rule with the second highest directionality ($CRW_{k=5}$) when non-habitat permeability was >0. In these cases, prevalence actually increased as habitats became more fragmented.

The effects of non-habitat permeability and move rules on prevalence depended on landscape parameters (Fig. 6). For example, when non-habitat was impermeable ($n = 0$), the SRW and CRW movement rules resulted in much higher prevalence than the PA rules. In this case, with some exceptions, the rule with the second highest directionality ($CRW_{k=5}$) resulted in the highest prevalence. However, when there was a large proportion of habitat ($p = 0.9$) and low habitat patchiness, the highest directionality ($CRW_{k=10}$) resulted in the highest prevalence. Also, when the proportion of habitat was low ($p = 0.1$ or 0.3) and habitat patchiness was high, the movement rule with the lowest directionality ($CRW_{k=2}$) resulted in higher prevalence than all other rules.

Prevalence also increased as the initial proportion of infective individuals (I_{init}) and the probability of transmission (P_{trans}) increased; however, the models showed no qualitative change in behavior as these parameters changed. These patterns may not hold though for diseases with more complex modes of transmission and host state transitions. These parameters had virtually no effect on the proportions of between-patch transmission and within-patch transmission.

Discussion

Our objectives were to design and build an ecological agent-based model of animal movement and infection transmission (the EID-ABM) as a "computational laboratory" to provide biological insights into the potential impacts of urban fragmentation on carnivore movement and disease spread. Using sensitivity analysis of the model responses, we addressed three specific questions regarding how the spread of an SI disease within and between habitat patches was affected by habitat fragmentation (i.e., landscape structure), movement behavior (i.e., move directionality), and the interaction of fragmentation and move behavior (i.e., degree of behavioral avoidance of the matrix between habitat fragments). From this relatively simple ABM—a directly transmitted pathogen with only susceptible and infected states and animals with basic movement behaviors—we observed complex and sometimes unexpected behavior.

For Question 1, our a priori expectation was that landscape fragmentation would increase contact rates and thus disease transmission within habitat patches (McCallum and Dobson 2002) and restrict dispersal and thus disease transmission between patches (Hess 1996). The sensitivity analysis results, however, revealed the opposite pattern; generally, within-patch transmission was lower, and between-patch transmission was higher, in more fragmented landscapes (i.e., those with a lower proportion of habitat and

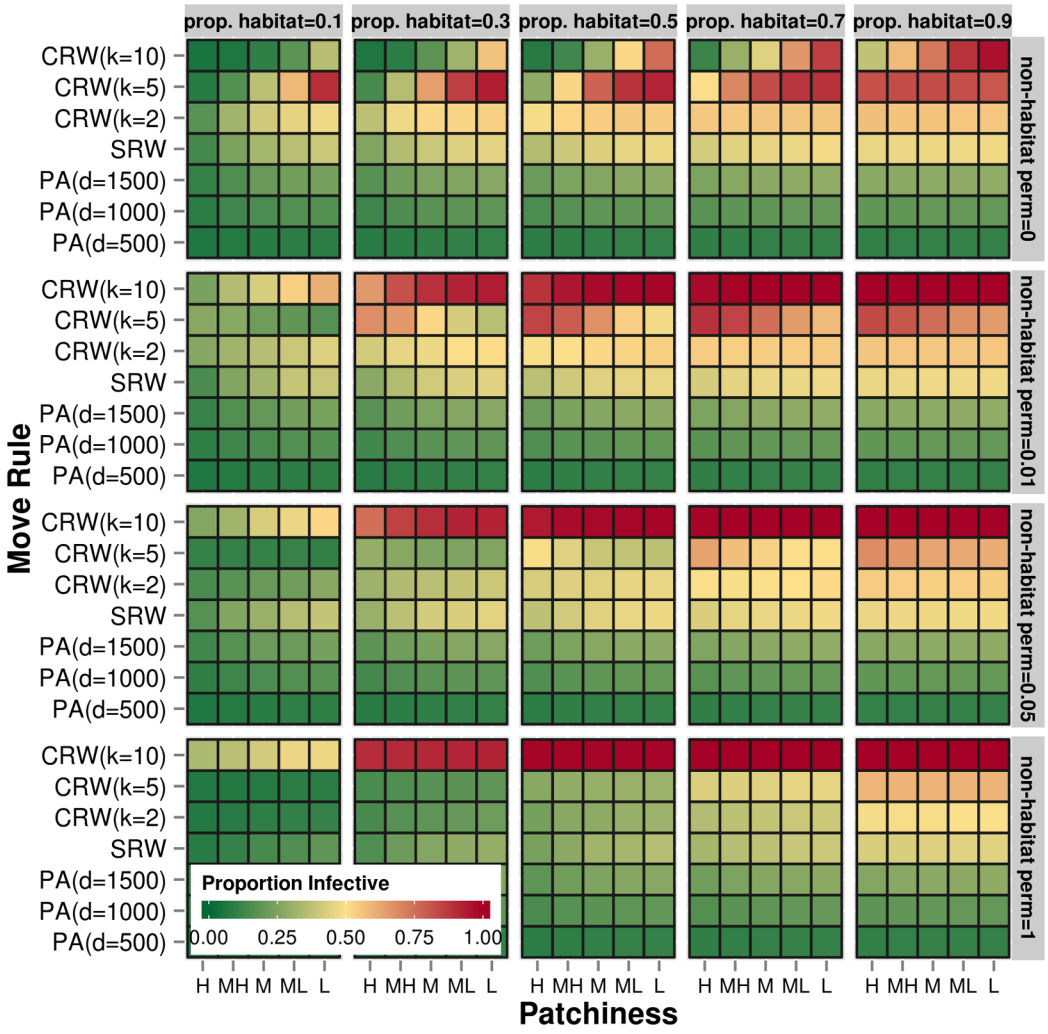

Fig. 6. Visual summaries of the sensitivity analysis results allow discovery of patterns in the behavior of the EID-ABM. This heat map shows the response of mean proportion infective at the final time step for 700 different parameter combinations (initial proportion of infective agents was 0.05 and probability of disease transmission was 0.1). The heat maps range from dark green, to yellow, to dark red with increasing mean proportion infective. There are 20 smaller heat maps nested within the larger figure. Each smaller heat map corresponds to a particular proportion of habitat (p, within columns) and non-habitat permeability (n, within rows). Within each smaller heat map, patchiness (the Hurst exponent) is varied on the x-axis, and is labeled by H (high patchiness, Hurst exponent = 0.1), MH (medium-high patchiness, Hurst exponent = 0.3), M (medium patchiness, Hurst exponent = 0.5), ML (medium-low patchiness, Hurst exponent = 0.7), and L (low patchiness, Hurst exponent = 0.9). The y-axis corresponds to the movement rules in increasing order of directionality from PA (point attraction) to SRW (simple random walk) to CRW (correlated random walk) rules. The parameters listed in parentheses alter the directionality of the movement rules. Relations shown diagrammatically in Fig. 4 and patterns illustrated in Figs. 5 and 7 were discovered using heat map visualizations like the one shown here. For our study area in coastal southern California, we estimated the proportion of habitat to be 0.3126 and the Hurst exponent to be 0.5845. Non-habitat permeability was low to very low for the bobcats in our study area (corresponding to the two middle rows). Resident bobcats were most consistent with move rule $PA_{d=1000}$, while dispersing bobcats were most consistent with rules $CRW_{k=3}$ or $CRW_{k=5}$.

more patchiness). In addition, overall disease prevalence (i.e., mean proportion infective at the last time step) typically was lower in more fragmented landscapes. Although it has been predicted that fragmented habitats isolate animals from disease transmission (Hess 1996), our ABM emphasizes that the capacity for disease transmission among patches is dependent upon the movement behavior of animals (Question 2), and how they respond to, and move within, the matrix between habitat fragments (Question 3).

As expected under Question 2, within-patch transmission was lower when movement was more directional, similar to that of a dispersing animal as compared to a resident animal with an established home range. Further, within-patch transmission increased as non-habitat became less permeable and animals avoided leaving habitat patches, consistent with predictions under Question 3. Patterns of between-patch transmission, however, were more complicated than initially predicted. As expected, if host animals were completely unable to disperse through the matrix, there was no between-patch disease transmission; although such isolation might reduce disease spread across the landscape, we emphasize that such lack of connectivity increases extinction probability of isolated populations due to a variety of deterministic and stochastic forces (McCallum and Dobson 2006). Contrary to predictions, however, the highest proportion of between-patch transmissions occurred at intermediate levels of both move directionality and non-habitat permeability. This was most evident with the second highest directionality (i.e., $CRW_{k=5}$) and when non-habitat permeability was low, but not zero (Fig. 7). In this case, the proportion of between-patch transmission events was highest compared to other movement rules with lesser or greater directionality (Fig. 7). Interestingly, non-habitat permeability interacted with habitat patchiness to influence overall disease prevalence. Although prevalence tended to decline as habitat patchiness increased (Fig. 6), changes in habitat patchiness had opposite effects on prevalence depending on non-habitat permeability for the $CRW_{k=5}$ movement rule (Fig. 7). With very low non-habitat permeability ($n = 0.01$), increasing patchiness led to increasing prevalence. In contrast, with no non-habitat permeability ($n = 0.0$), increasing patchiness led to decreasing prevalence.

In summary, the results for this movement rule, which correspond to a dispersing animal, include: (1) the highest proportions of between-patch transmissions, which indicates that animals with this movement behavior were very effective at carrying the infection between habitat patches, (2) higher infection prevalence when non-habitat was impermeable, (3) a qualitatively different response to changes in habitat patchiness compared to other movement rules, and (4) a greater range of prevalence outcomes as the proportion and patchiness of habitat changed. This qualitative change in behavior suggests that it may be possible under some conditions for increasing habitat patchiness (while keeping the proportion of habitat constant) to increase the spread of an infection across a landscape. In the EID-ABM, this qualitative change in system-level behavior was strictly due to agent-level changes in movement behavior. Our models therefore reveal that host movement behavior can produce unanticipated outcomes in the spread of an infection across a landscape, with the potential for critical thresholds related to movement behavior that alter disease dynamics.

The EID-ABM results have important implications for disease dynamics of mammalian carnivores in urbanizing landscapes. Our models predict that dispersing animals willing to risk movement into non-habitat, and those engaged in more directional movement, are likely to transmit disease to animals in other patches, leading to increased transmission of infections between wildlife, domestic animals, and humans along and within the urban matrix surrounding habitat fragments. Importantly, however, our models predict that if the matrix between habitat fragments is somewhat permeable to animal movement, which might be the case for all but the most fragmentation-sensitive species, then high rates of between-patch disease transmission can result, even in highly fragmented landscapes. Bobcats in southern California tend to avoid urban areas, but will occasionally navigate across the urban matrix to visit disjunct habitat patches (Crooks 2002, Riley et al. 2003, Riley et al. 2010, Tracey et al. 2013). As such, the actual permeability of the urban matrix in coastal southern California for bobcats is most consistent with the very low to low classification of non-habitat

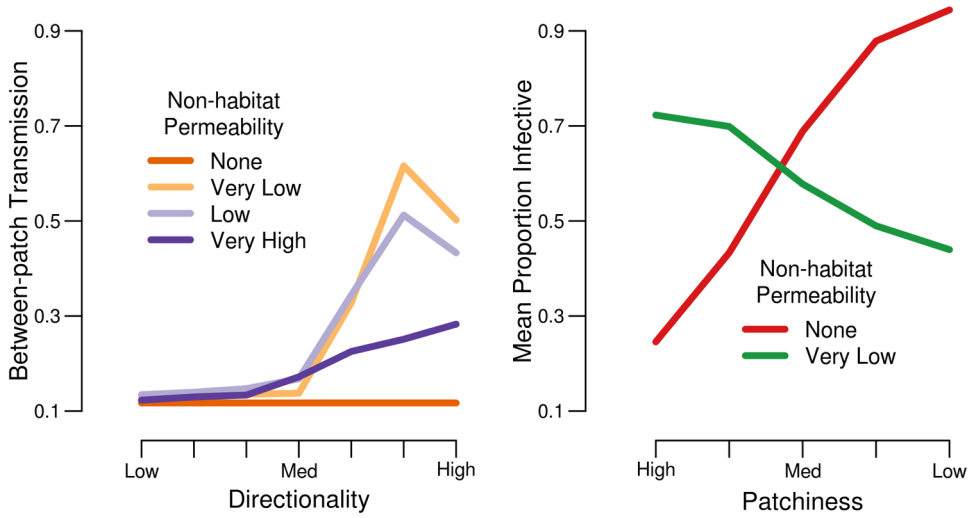

Fig. 7. EID-ABM yielded non-linear, counter-intuitive results. The left plot illustrates the simulation results for the proportion of between-patch transmission events (y-axis) versus movement rule directionality (x-axis) for each value of non-habitat permeability. These results occurred for a landscape with high patchiness ($H = 0.01$). Between-patch transmission was highest for the movement rule with the second highest directionality ($CRW_{k=5}$) with very low non-habitat permeability ($n = 0.01$). The right plot shows the mean proportion infective at the final time step (y-axis) versus habitat patchiness (x-axis) for movement rule $CRW_{k=5}$. Note that decreasing habitat patchiness has opposing effects depending on whether there is no non-habitat permeability ($n = 0.0$, red line) or very low non-habitat permeability ($n = 0.01$, green line). In both plots, proportion habitat (p) was 0.3, proportion of initially infective agents was 0.05, and the probability of disease transmission was 0.1. Our study area was characterized by medium patchiness, moderate directionality (for dispersing individuals), and very low to low non-habitat permeability.

permeability in our models (Tracey et al. 2013). GPS-collared bobcats in southern California typically engage in movement behavior that is consistent with point attraction (e.g., the $PA_{d=1000}$ rule) if they are residents or directional movement (e.g., the $CRW_{k=5}$ rule) if they are dispersers (Tracey et al. 2013; *unpublished data*). In our models, point attraction had the lowest between-patch transmission rates, the highest within-patch transmission rates, and the lowest overall prevalence (Figs. 4 and 6). In contrast, directional movement (CRW $k = 5$) yielded high between-patch transmission, low within-patch transmission, and moderate overall prevalence (Figs. 4 and 6). This was particularly the case when our simulated landscapes had levels of fragmentation similar to the actual landscape in our coastal southern California field site (study area, $p = 0.3126$, $H = 0.5845$; simulation scenario, $p = 0.3$ and $H = 0.5$). Because the resident and disperser movement behaviors are related to the adult and sub-adult life history stages, the proportion of individuals engaged in each depends on the age structure of the populations and the availability of suitable areas to establish home ranges.

Our findings regarding between-patch disease transmission are also consistent with FIV transmission among bobcats across the urban landscape of coastal southern California (Lee et al. 2012). Although gene flow is restricted between two subpopulations of animals on either side of the Interstate 5 (I-5) freeway and associated urban development in Orange County, south of Los Angeles, FIV phylogenetic analyses document frequent viral transmissions among these two subpopulations. This is in contrast to comparisons of FIV isolates north and south of Los Angeles, which segregate distinctly by geographic area. Thus, while the city of Los Angeles represents a seemingly impermeable barrier to both bobcat movement and disease transmission, the I-5 freeway complex is appar-

ently somewhat permeable to the movement of bobcats and their diseases, thus allowing occasional between-patch transmission. The fact that host gene flow is restricted between these subpopulations, while viral transmission is not, may indicate that animals moving from one side of the highway to the other have a low success rate at establishing breeding territories and passing on their genetic material (Lee et al. 2012)—consistent with our model predictions of disease transmission by 'risk-taking dispersers.'

When developing modeling approaches, we believe it is essential to start with a simple model, understand its behavior, and then incrementally increase the level of detail. For this reason we have omitted demography, life history, social interaction, and adaptation from our current models. Models that incorporate more details of the dispersal process, such as behavior and social rank, will provide additional insights into the spread of disease (Pontier et al. 1998, Fromont et al. 2003). Some of these features have been examined here, but future models should account for sex, age, and life-history stages because these can strongly influence movement patterns and thus disease transmission dynamics in a fragmented landscape. For example, sub-adult felids often disperse to establish territories away from natal areas (Winegarner and Winegarner 1982, Logan and Sweanor 2001) and would therefore influence disease transmission differently than adult animals. This is also the population typically newly exposed to FIV, as seroconversion increases substantially with age (Biek et al. 2003, VandeWoude and Apetrei 2006, Bevins et al. 2012). Likewise, another retroviral disease of domestic cats, feline leukemia virus (FeLV), is extremely sensitive to dispersal rate as well as to sex and age class of individuals dispersing (Fromont et al. 1996). Animals of different sex or age classes are also likely to respond differently to urban landscapes. Adult females bobcats are less likely to venture into urban areas than male or young female bobcats (Riley et al. 2003), and disease transmission among these animals would be predicted to be markedly different, similar to the effects of non-habitat permeability on pathogen spread in our EID-ABM. In addition, urban carnivores often suffer age- and sex-specific mortality (e.g., due to vehicle collisions or human persecution while dispersing) that may lead to population structures that differ from rural carnivores (Tigas et al. 2002, Riley et al. 2003) and thus potentially altered disease dynamics. Future work should explore the influence of movement and social behavior associated with these individual-level states on the spread of pathogens in conjunction with anthropogenic mortality.

Some of the other pathogens we are currently studying, such as *Toxoplasma gondii* and *Yersinia pestis* (Bevins et al. 2009, Bevins et al. 2012), infect multiple host species, and species-specific differences in movement behavior also may have considerable effects on disease dynamics. For example, one study showed that urban bobcats were limited to park habitats and rarely ventured into residential areas, whereas gray foxes (*Urocyon cinereoargenteus*) often traveled into the urban matrix and were more likely to be infected with canine parvovirus, putatively following increased contacts with domestic animals shedding this virus (Riley et al. 2004). Coyotes (*Canis latrans*) are also more likely to encroach into urban areas than bobcats (Crooks 2002, Riley et al. 2003). In general, carnivores vary considerably in their sensitivity to habitat fragmentation, which can result in transformations of the structure and composition of carnivore communities, and their prey, in urban systems (Crooks 2002). Such community-level impacts of habitat fragmentation are also likely to affect the spread of pathogens. Thus, another important question for future ABM work is to explore the consequences of having multiple species involved in the transmission cycle of a single pathogen.

An advantage of the ABM approach is that model outputs are produced at different levels of organization from the agent (or individual organism) level up to the population (or system) level. Using a pattern-oriented modeling (Grimm et al. 2005), these outputs provide multiple points of comparison between the ABMs and the real-world system. As natural habitats become increasingly fragmented, and as contacts between humans, wildlife, and domestic animals continue to rise, the need to understand the pathogens that move between them will become increasingly important. As our work demonstrates, ABM is a useful tool for investigating the potential behavior of these systems.

Acknowledgments

We thank E. Boydston, R. Fisher, and L. Lyren for their collaboration on field research of bobcats in southern California, and M. Lappin and M. Salman for their input on the disease component of the study. Additional information on model design and implementation is available from the authors. Any use of trade, product, or firm names is for descriptive purposes only and does not imply an endorsement by the US Government. This study was supported by NSF Ecology of Infectious Disease research program (NSF EF-0723676). The funders had no role in study design, data collection and analysis, decision to publish, or preparation of the manuscript.

Literature Cited

Auchincloss, A. H., and A. V. Diez Roux. 2008. A new tool for epidemiology: the usefulness of dynamic-agent models in understanding place effects on health. American Journal of Epidemiology 168:1–8.

Bankes, S. C. 2002. Agent-based modeling: a revolution? Proceedings of the National Academy of Sciences USA 99 Supplement 3:7199–7200.

Bevins, S. N., S. Carver, E. E. Boydston, L. M. Lyren, M. Alldredge, K. A. Logan, S. P. D. Riley, R. N. Fisher, T. W. Vickers, W. Boyce, M. Salman, M. R. Lappin, K. R. Crooks, and S. VandeWoude. 2012. Three pathogens in sympatric populations of pumas, bobcats, and domestic cats: implications for infectious disease transmission. PLoS ONE 7:e31403.

Bevins, S. N., J. A. Tracey, S. P. Franklin, V. L. Schmit, M. L. Macmillan, K. L. Gage, M. E. Schriefer, K. A. Logan, L. L. Sweanor, M. W. Alldredge, C. Krumm, W. M. Boyce, W. Vickers, S. P. Riley, L. M. Lyren, E. E. Boydston, R. N. Fisher, M. E. Roelke, M. Salman, K. R. Crooks, and S. VandeWoude. 2009. Wild felids as hosts for human plague, western United States. Emerging Infectious Diseases 15:2021–2024.

Biek, R., A. G. Rodrigo, D. Holley, A. Drummond, C. R. Anderson, Jr., H. A. Ross, and M. Poss. 2003. Epidemiology, genetic diversity, and evolution of endemic feline immunodeficiency virus in a population of wild cougars. Journal of Virology 77:9578–9589.

Biek, R., T. K. Ruth, K. M. Murphy, C. R. Anderson, and M. Poss. 2006. Examining effects of persistent retroviral infection on fitness and pathogen susceptibility in a natural feline host. Canadian Journal of Zoology 84:365–373.

Courchamp, F., L. Say, and D. Pontier. 2000. Transmission of feline immunodeficiency virus in a population of cats (*Felis catus*). Wildlife Research 27:603–611.

Crooks, K. R. 2002. Relative sensitivities of mammalian carnivores to habitat fragmentation. Conservation Biology 16:488–502.

Crooks, K. R., and M. Sanjayan. 2006. Connectivity conservation. Cambridge University Press, New York, New York, USA.

Fa, J. E., C. M. Sharples, D. J. Bell, and D. DeAngelis. 2001. An individual-based model of rabbit viral haemorrhagic disease in European wild rabbits (*Oryctolagus cuniculus*). Ecological Modelling 144:121–138.

Franklin, S. P., J. L. Troyer, J. A. TerWee, L. M. Lyren, W. M. Boyce, S. P. D. Riley, M. E. Roelke, K. R. Crooks, and S. VandeWoude. 2007. Frequent transmission of immunodeficiency viruses among bobcats and pumas. Journal of Virology 81:10961–10969.

Fromont, E., M. Artois, and D. Pontier. 1996. Cat population structure and circulation of feline viruses. Acta Oecologia 17:609–620.

Fromont, E., D. Pontier, and M. Langlais. 2003. Disease propagation in connected host populations with density-dependent dynamics: the case of the feline leukemia virus. Journal of Theoretical Biology 223:465–475.

Gimblett, H. R. 2002. Integrating geographic information systems and agent-based modeling techniques for simulating social and ecological processes. Oxford University Press, New York, New York, USA.

Green, J. L., A. Hastings, P. Arzberger, F. J. Ayala, K. L. Cottingham, K. Cuddington, F. Davis, J. A. Dunne, M. J. Fortin, L. Gerber, and M. Neubert. 2005. Complexity in ecology and conservation: Mathematical, statistical, and computational challenges. BioScience 55:501–510.

Grenfell, B. T., and A. P. Dobson. 1995. Ecology of infectious diseases in natural populations. Cambridge University Press, New York, New York, USA.

Grimm, V., E. Revilla, U. Berger, F. Jeltsch, W. M. Mooij, S. F. Railsback, H. H. Thulke, J. Weiner, T. Wiegand, and D. L. DeAngelis. 2005. Pattern-oriented modeling of agent-based complex systems: lessons from ecology. Science 310:987–991.

Gustafson, E. J., and R. H. Gardner. 1996. The effect of landscape heterogeneity on the probability of patch colonization. Ecology 77:94–107.

Hess, G. 1996. Disease in metapopulation models: Implications for conservation. Ecology 77:1617–1632.

Homer, C., C. Huang, L. Yang, B. Wylie, and M. Coan. 2004. Development of a 2001 National Landcover Database for the United States. Photogrammetric Engineering and Remote Sensing 70:829–840.

Jeltsch, F., M. S. Müller, V. Grimm, C. Wissel, and R. Brandl. 1997. Pattern formation triggered by rare

events: lessons from the spread of rabies. Proceedings of the Royal Society B 264:495–503.

Jones, K. E., N. G. Patel, M. A. Levy, A. Storeygard, D. Balk, J. L. Gittleman, and P. Daszak. 2008. Global trends in emerging infectious diseases. Nature 451:990–993.

Laurenson, K., C. Sillero-Zubiri, H. Thompson, F. Shiferaw, S. Thirgood, and J. Malcolm. 1998. Disease as a threat to endangered species: Ethiopian wolves, domestic dogs and canine pathogens. Animal Conservation 1:273–280.

Lee, J. S., E. W. Ruell, E. E. Boydston, L. M. Lyren, R. S. Alonso, J. L. Troyer, K. R. Crooks, and S. U. E. VandeWoude. 2012. Gene flow and pathogen transmission among bobcats (*Lynx rufus*) in a fragmented urban landscape. Molecular Ecology 21:1617–1631.

Logan, K. A., and L. L. Sweanor. 2001. Desert puma: evolutionary ecology and conservation of an enduring carnivore. Island Press, Washington, D.C., USA.

LoGiudice, K., R. S. Ostfeld, K. A. Schmidt, and F. Keesing. 2003. The ecology of infectious disease: Effects of host diversity and community composition on Lyme disease risk. Proceedings of the National Academy of Sciences USA 100:567–571.

McCallum, H., and A. Dobson. 2002. Disease, habitat fragmentation and conservation. Proceedings of the Royal Society B 269:2041–2049.

McCallum, H., and A. Dobson. 2006. Disease and connectivity. Page 732 *in* K. R. Crooks and M. Sanjayan, editors. Connectivity conservation. Cambridge University Press, New York, New York, USA.

McDonald, R. I., P. Kareiva, and R. T. Forman. 2008. The implications of current and future urbanization for global protected areas and biodiversity conservation. Biological Conservation 141:1695–1703.

McKinney, M. L. 2002. Urbanization, Biodiversity, and Conservation The impacts of urbanization on native species are poorly studied, but educating a highly urbanized human population about these impacts can greatly improve species conservation in all ecosystems. BioScience 52:883–890.

Picquet, M., J. C. Ernould, J. Vercruysse, V. R. Southgate, A. Mbaye, B. Sambou, M. Niang, and D. Rollinson. 1996. The epidemiology of human schistosomiasis in the Senegal river basin. Transactions of the Royal Society of Tropical Medicine and Hygiene 90:340–346.

Pontier, D., E. Fromont, F. Courchamp, M. Artois, and N. G. Yoccoz. 1998. Retroviruses and sexual size dimorphism in domestic cats (*Felis catus* L.). Proceedings of the Royal Society B 265:167–173.

R Development Core Team. 2007. R: a language and environment for statistical computing. R Development Core Team, Vienna, Austria.

Riley, S. P., E. E. Boydston, K. R. Crooks, and L. M. Lyren. 2010. Bobcats (*Lynx rufus*). *In* S. D. Gehrt, S. P. Riley, and B. L. Cypher, editors. Urban carnivores: ecology, conflict, and conservation. Johns Hopkins University Press, Baltimore, Maryland, USA.

Riley, S. P. D. 2006. Spatial ecology of bobcats and gray foxes in urban and rural zones of a national park. Journal of Wildlife Management 70:1425–1435.

Riley, S. P. D., J. Foley, and B. Chomel. 2004. Exposure to feline and canine pathogens in bobcats and gray foxes in urban and rural zones of a National Park in California. Journal of Wildlife Diseases 40:11–22.

Riley, S. P. D., R. M. Sauvajot, T. K. Fuller, E. C. York, D. A. Kamradt, C. Bromley, and R. K. Wayne. 2003. Effects of urbanization and habitat fragmentation on bobcats and coyotes in southern California. Conservation Biology 17:566–576.

Ruell, E. W., S. P. D. Riley, M. R. Douglas, J. P. Pollinger, and K. R. Crooks. 2009. Estimating bobcat population sizes and densities in a fragmented urban landscape using noninvasive capture-recapture sampling. Journal of Mammalogy 90:129–135.

Smith, K. F., K. Acevedo-Whitehouse, and A. B. Pedersen. 2009. The role of infectious diseases in biological conservation. Animal Conservation 12:1–12.

Stauffer, D., and A. Aharony. 1994. Introduction to percolation theory. Taylor & Francis, London, UK.

Thulke, H. H., V. Grimm, M. S. Müller, C. Staubach, L. Tischendorf, C. Wissel, and F. Jeltsch. 1999. From pattern to practice: a scaling-down strategy for spatially explicit modelling illustrated by the spread and control of rabies. Ecological Modelling 117:179–202.

Tigas, L. A., D. H. Van Vuren, and R. M. Sauvajot. 2002. Behavioral responses of bobcats and coyotes to habitat fragmentation and corridors in an urban environment. Biological Conservation 108:299–306.

Tracey, J. A., J. Zhu, E. Boydston, L. Lyren, R. N. Fisher, and K. R. Crooks. 2013. Mapping behavioral landscapes for animal movement: a finite mixture modeling approach. Ecological Applications 23:654–669.

Troyer, J. L., J. Pecon-Slattery, M. E. Roelke, W. Johnson, S. VandeWoude, N. Vazquez-Salat, M. Brown, L. Frank, R. Woodroffe, C. Winterbach, H. Winterbach, G. Hemson, M. Bush, K. A. Alexander, E. Revilla, and S. J. O'Brien. 2005. Seroprevalence and genomic divergence of circulating strains of feline immunodeficiency virus among Felidae and Hyaenidae species. Journal of Virology 79:8282–8294.

Turner, M. G., R. H. Gardner, and R. V. O'Neill. 2001. Landscape ecology in theory and practice: pattern and process. Springer, New York, New York, USA.

Valbuena, D., P. H. Verburg, A. K. Bregt, and A.

Ligtenberg. 2009. An agent-based approach to model land-use change at a regional scale Landscape Ecology.
VanDerWal, J., L. Falconi, S. Januchowski, L. Shoo, and C. Storlie. 2012. SDMTools: species distribution modelling tools: tools for processing data associated with species distribution modelling exercises. R package version 1.1-13. http://cran.r-project.org/web/packages/SDMTools/index.html
VandeWoude, S., and C. Apetrei. 2006. Going wild: Lessons from naturally occurring T-lymphotropic lentiviruses. Clinical Microbiology Reviews 19:728–762.
Vittor, A. Y., W. Pan, R. H. Gilman, J. Tielsch, G. Glass, T. Shields, W. Sanchez-Lozano, V. V. Pinedo, E. Salas-Cobos, S. Flores, and J. A. Patz. 2009. Linking deforestation to malaria in the Amazon: characterization of the breeding habitat of the principal malaria vector, *Anopheles darlingi*. American Journal of Tropical Medicine and Hygiene 81:5–12.
Wickham, H. 2009. ggplot2 elegant graphics for data analysis. Springer, New York, New York, USA.
Williams, E. S., E. T. Thorne, M. J. G. Appel, and D. W. Belitsky. 1988. Canine-distemper in black-footed ferrets (*Mustela nigripes*) from Wyoming. Journal of Wildlife Diseases 24:385–398.
Winegarner, C. E., and M. S. Winegarner. 1982. Reproductive history of a bobcat. Journal of Mammalogy 63:680–682.
Woolhouse, M. E. J., and S. Gowtage-Sequeria. 2005. Host range and emerging and reemerging pathogens. Emerging Infectious Diseases 11:1842–1847.
Zollner, P. A., and S. L. Lima. 1999. Search strategies for landscape-level interpatch movements. Ecology 80:1019–1030.

Supplemental Material

Appendix A

Additional details on movement rules

The cells in an agent's neighborhood are indexed $i = 1, ..., 9$, which correspond to the directions E, NE, N, NW, W, SW, S, SE, and *C*, where *C* indicates the cell currently occupied by the agent. At time t, the agent is located at coordinates (x_t, y_t); therefore, its initial location is (x_0, y_0). The probability of moving to cell i at time t, $p_{i,t}$, is given by:

$$p_{i,t} = \frac{q_{i,t}}{\sum_{j=1}^{9} q_{j,t}}$$

where $q_{i,t}$ is the probability potential for cell i at time t (similar to Gustafson and Gardner 1996). The probability potential is calculated as the product of three factors:

$$q_{i,t} = C(A_i) \times P(h_i) \times P_t(A_i)$$

where A_i is the angle from the agent's current cell to neighboring cell i (which is undefined for $i = 9$), $C(A_i)$ is an angle correction factor, h_i is the habitat type of cell i, $P(h_i)$ is the preference for the habitat type of cell i, and $P_t(A_i)$ is the preference for the angle A_i at time t. $C(A_i) = 1$ if A_i is a diagonal move and $\sqrt{2}$ otherwise. $P(h_i) = \{1$ if h_i = habitat; n if h_i = non-habitat$\}$. $P_t(A_i)$ depends on the move behavior rule.

- For the simple random walk (SRW), $P_t(A_i) = 1$ for all i and t.
- For the correlated random walk (CRW), $P_t(A_i) = \exp(k[\cos(A_i - A_t) - 1])$, where k is a fixed concentration parameter, which controls the strength of the tendency to move in the preferred angle $A_t = \text{atan2}(y_t - y_{t-1}, x_t - x_{t-1})$, which is the angle of the move at the previous time step.
- For the point attraction movement rule (PA), $P_t(A_i) = \exp(k_t[\cos(A_i - A_t) - 1])$, where $A_t = \text{atan2}(y_0 - y_t, x_0 - x_t)$ is the angle from the current location to the agent's initial location which serves as the center of its home range. The concentration parameter k_t, which controls the strength of the agent's tendency to move toward the

preferred angle, is given by the logistic function $k_t = [k_{\max} \exp(b[D_t - d])/[1 + \exp(b[D_t - d])]$. The parameter $k_{\max}$ is the maximum concentration. $D_j = \text{sqrt}([x_0 - x_t]^2 + [y_0 - y_t]^2)$ is the distance from the agent's location at time t to the center of its home range. Generally, k_t increases to $k_{\max}$ as the agent moves away from the center if its home range, and decreases to 0 as it moves toward it. The parameter d is the inflection point of the logistic function, which is roughly the radius of the agent's home range. The parameter b controls the steepness of the logistic function as the agent moves away from the center of its home range.

These equations provide the angle preference for movement to neighboring cells ($i = 1, ..., 8$). $P_t(A_i)$ for the current cell is computed as the average of the $P_t(A_i)$ for the eight neighboring cells.

Appendix B

Comparison of Southern California land cover and fractal landscapes used in the EID-ABM

Using a land cover raster for our study area, we computed the proportion of habitat (defined as land cover that was not water, urban, or roads) and then used the SDMTools package in R to compute the fractal dimension index D and Hurst exponent ($H \approx 2 - D$) of the habitat patches. This resulted in the estimates $p = 0.3125825$ and $H = 0.584515$ for the land cover data from our study area.

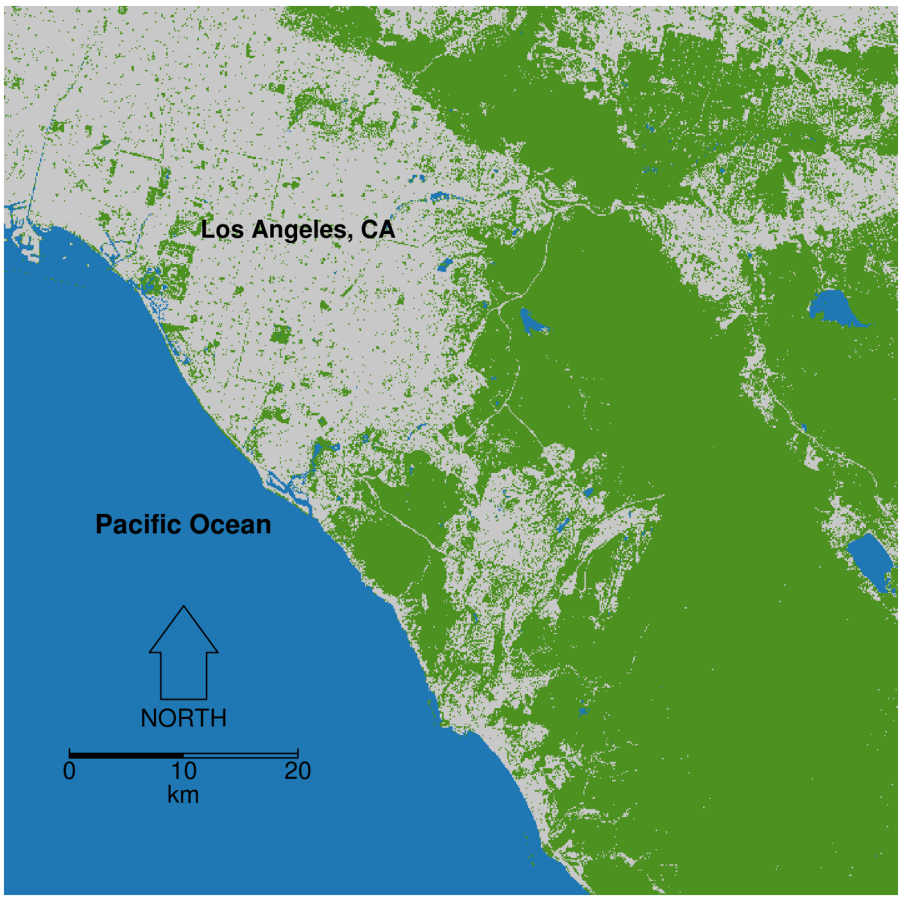

Fig. B1. Land cover data for our study area that include parts of San Diego, Orange, and Los Angeles Counties of southern California. Water is in blue, urban is in gray, and other land cover is in green.

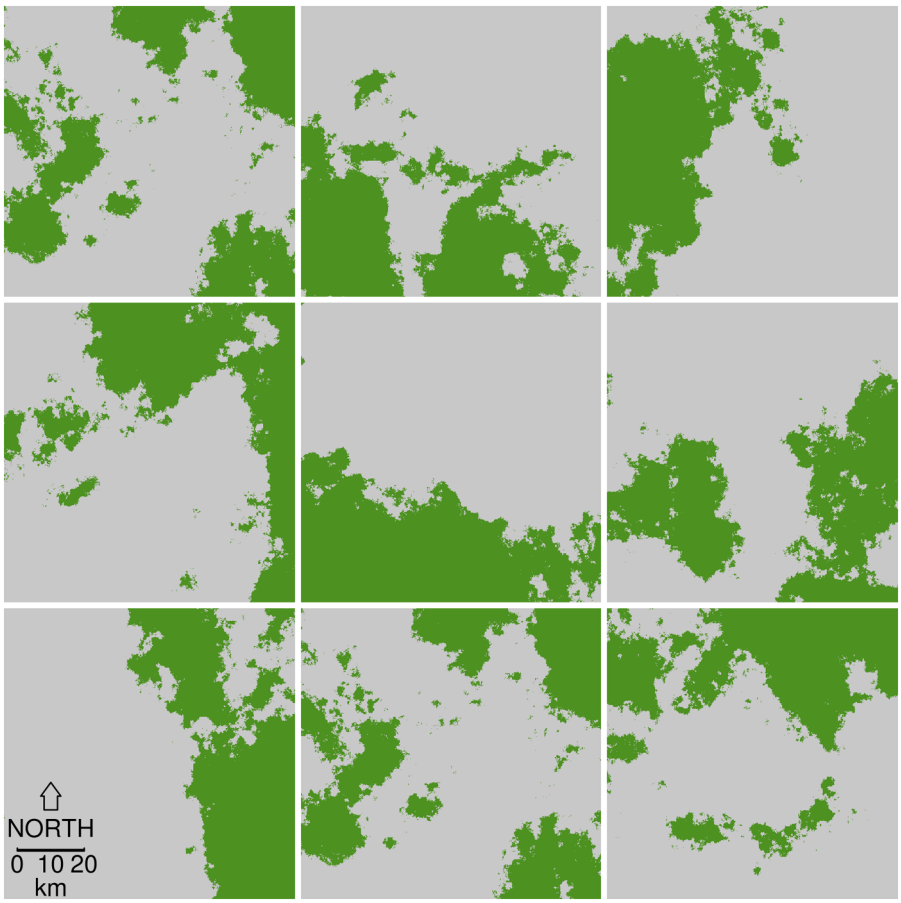

Fig. B2. Examples of nine fractal landscapes created using the same code used to create the fractal landscapes in the EID-ABM and the parameters estimated from land cover in our study area. Habitat is in green and non-habitat is in gray.

Supplement

Binary landscape raster for study area and Java source code for the EID-ABM (*Ecological Archives* C005-011-S1).